A new approach to determine and quantify structural units in silicate glasses using micro-reflectance Fourier-Transform infrared spectroscopy

KIM N. DALBY* AND PENELOPE L. KING

Department of Earth Sciences, The University of Western Ontario, London, Ontario N6A 5B7, Canada

ABSTRACT

Eight silicate unit vibrational modes were identified in a suite of PbO-SiO_2 glasses using micro-reflectance Fourier Transform infrared (µR-FTIR) spectra that were transformed using the Kramers-Kronig relation. The transformed FTIR spectra, in the 800–1200 cm^{-1} range, were deconvolved systematically into eight Voigt-shaped bands at centers that were predicted from the second derivative of the spectra. The area of the eight bands varied as a function of SiO_2 content, and these trends were combined with theoretical constraints to identify and assign the bands to seven provisional silicate units: SiO_4^{4-} (830 and 860 cm^{-1}), $Si_2O_7^{6-}$ (900 cm^{-1}), $Si_6O_{18}^{12-}$ (950 cm^{-1}), $Si_2O_6^{4-}$ (980 cm^{-1}), $Si_4O_{11}^{6-}$ (1010 cm^{-1}), $Si_2O_5^{2-}$ (1050 cm^{-1}), and SiO_2 (1100 cm^{-1}). The provisional units were then grouped according to their NBO/T values: NBO/T = 4 (SiO_4^{4-}), NBO/T = 3 ($Si_2O_7^{6-}$), NBO/T = 2 ($Si_6O_{18}^{12-}$ and $Si_2O_6^{4-}$), NBO/T = 1 ($Si_4O_{11}^{6-}$ and $Si_2O_5^{2-}$) and NBO/T = 0 (SiO_2). The derived quantities of each NBO/T unit compare favorably with nuclear magnetic resonance data for PbO-SiO_2 glasses reported in the literature. This new approach for determining glass structure is advantageous because it may be performed on small Fe-bearing samples with minimal preparation, and analyses are rapid and relatively inexpensive.

Keywords: IR spectroscopy, glass structure, band fitting, PbO-SiO_2

INTRODUCTION

Theoretical models propose that the structure of silicate glass is dominated by discrete silicate units with short-to-medium-range order, and that the physiochemical properties of silicate glasses are controlled by the relative percentage of these co-existing silicate units (Bell et al. 1968; Hess 1975; Masson et al. 1970; McMillan and Wolf 1995; Mysen et al. 1982b; Nesbitt and Fleet 1981; Toop and Samis 1962). Therefore, to understand the behavior of silicate glasses it is necessary to identify and quantify the silicate units that contribute to their short- to medium-range structure. Spectroscopic techniques such as nuclear magnetic resonance (NMR), X-ray absorption fine structure (XAFS), neutron diffraction, and Raman spectroscopy have been used previously to characterize the structural units in silicate glasses (Bessada et al. 1994; Cormier et al. 1996; Fayon et al. 1998, 1999; Poe et al. 1992; Rybicki et al. 2001; Stebbins 1995). To provide a more complete inventory and understanding of the structural units in silicate glasses, a method for identifying and quantifying structural units from infrared (IR) data is discussed.

The structural units in silicate glasses are commonly modeled using the silicate units found in crystals (e.g., minerals; Fig. 1). The silicate units in crystals are a subgroup of the structural units and they are grouped according to their ratio of non-bridging oxygen per network forming tetrahedra (NBO/T) to provide a measure of their polymerization (Fig. 1; Heaton and Moore 1957; Hess 1989; McMillan and Wolf 1995; Mysen et al. 1982b). However, the bulk silicate glass typically contains more than one structural unit; for example, five silicate units are identified in

many studies (e.g., Stebbins 1995; Fig. 1 and Table 1a). Therefore, the bulk NBO/T of a glass is used to indicate its average polymerization state, such that a silicate glass with a low NBO/T has a highly polymerized structure presumably dominated by silicate units with low NBO/T (Fig. 1).

Silicate units may be detected using vibrational spectroscopy because they each have a distinct molecular geometry that will scatter, emit, and/or absorb light at a discrete frequency. In the case of Raman spectroscopy, silicate units are detected if their polarizability changes when they are subject to one vibrational quantum of energy (Herzberg 1945). Thus Raman spectra of silicate glasses may be "deconvolved" into discrete structural units. We use the term "deconvolve" in this study to describe this process although we recognize that strictly "deconvolve" refers to a mathematical function (Hawthorne and Waychunas 1988). In contrast, with IR spectroscopy the silicate units are detected when their dipole moment changes as they are subject to incoming energy at the resonant vibrational frequency. Yet IR spectra are not commonly "deconvolved" into discrete structural units.

This paper details a method for resolving individual Voigt-shaped bands from micro-reflectance Fourier Transform IR (µR-FTIR) spectra that have been transformed into absorbance spectra, with the primary goal of identifying specific silicate unit vibrations. The position and number of the bands to use in any fitting process may be identified using a model-independent or model-dependent process. In a model-independent fit, the bands are added arbitrarily to maximize a goodness of fit and are subsequently assigned to silicate units based on previous work. In a model-dependent fit, bands are added at positions predicted for silicate units from empirical crystal chemical calculations. In the proposed model we combine the two approaches by systematically adding bands at centers predicted from the second
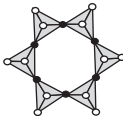
* E-mail: kdalby@uwo.ca
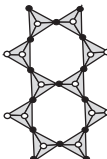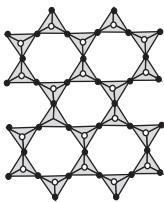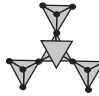
Anionic unit	SiO_4^{4-}	$Si_2O_7^{6-}$	$Si_6O_{18}^{12-}$	$Si_2O_6^{4-}$	$Si_4O_{11}^{6-}$	$Si_2O_5^{2-}$	SiO_2
Silicate subclass	Isolated tetrahedra	Paired tetrahedra	Ring	Chain	Double chain	Sheet	Framework
NBO/T	4	3	2	2	1 or 2	1	0
Approx. Raman band (cm^{-1})	790–850	890–950	-	930–1000	-	1020–1100	1150–1200 1060–1070

○ NBO
● BO
△ Silicon Tetrahedra

FIGURE 1. Nomenclature and structures of seven silicate units found in crystals. The least polymerized unit has four non-bridging oxygen (NBO) per silicate tetrahedra (T). With increasing polymerization, the NBO/T decreases due to the formation of more bridging oxygen (BO). These silicate units are commonly used to describe glass structure and the approximate wavenumber (cm^{-1}) of the vibration of the units observed in Raman studies is given (from Furukawa et al. 1978, 1981; McMillan 1984; McMillan and Wolf 1995; Mysen et al. 1982a, 1982b; Piriou and Arashi 1980).

TABLE 1. Band positions and assignments of vibrational modes of silicate units from previous deconvolved infrared (IR) and Raman (R) spectra: (a) in glasses and, (b) crystals*

(a) Glasses

Silicate unit	SiO_4^{4-}	$Si_2O_7^{6-}$	N/A	$Si_2O_6^{4-}$	N/A	$Si_2O_5^{2-}$	SiO_2	Ref.
NBO/T	4	3		2		1	0	
	cm^{-1}	cm^{-1}	cm^{-1}	cm^{-1}	cm^{-1}	cm^{-1}	cm^{-1}	
Calcium silicate (R)	861 ν_s	–	1010	956 ν_s	1050	1100–1058 ν_s	1150–1200 ν_s	1
Alkali silicate (R)	850 ν_s	900 ν_s	–	950 ν_s	1060	1090 ν_s	1150–1200 ν_s	2
Alkali/alkaline earth (R)	850 ν_s	900 ν_s	–	1000–950 ν_s	-	1100–1050 ν_s	1060, 1200 ν_{as}	3
Alkali/alkaline earth (R)	850 ν_s	900 ν_s	–	1000 ν_s	-	1100–1050 ν_s	1060, 1200 (1100) ν_s	4
Lead silicate (R)	840	950	–	–	-	1020	–	5
Lead silicate (R/IR)	825 ν_s	–	–	950	-	1100	1070, 1190	6
Alkali silicate (IR)	800–900 ν_{as}	–	–	1050 ν_{as}	-	1075 ν_{as}	1060, 1150 ν_{as}	4

(b) Crystals (~cm^{-1})

Silicate unit	SiO_4^{4-}	$Si_2O_7^{6-}$	$Si_6O_{18}^{12-}$	$Si_2O_6^{4-}$	$Si_4O_{11}^{6-}$	$Si_2O_5^{2-}$	SiO_2	Ref.
NBO/T	4	3	2	2	1 (and 2)	1	0	
cm^{-1}								
1100					ν_{as} Si-O-Si (Vs)		ν_{as} Si-O-Si (Vs)	7
1050		ν_{as} Si-O-Si (c)		ν_{as}' Si-O-Si (s)	ν_{as} Si-O-Si (s)	ν_{as} Si-O-Si (Vs)		7
1010			ν_{as} Si-O-Si (s)	ν_{as} Si-O-Si (s)	ν_{as} Si-O-Si (Vs)			7
980				ν_{as} Si-O-Si (s)				7
950			ν_{as} O-Si-O (Vs)		ν_{as} O-Si-O (Vs)			7
900	ν_{as} SiO$_4$ (c)	ν_{as} SiO$_3$ (c)						7
860	ν_{as} SiO$_4$ (c)							7
830	ν_s SiO$_4$ (N/A)							8, 9

Notes: 1 = Mysen et al. 1982a; 2 = Mysen et al. 1982b; 3 = McMillan 1984; 4 = McMillan and Wolf 1995; 5 = Furukawa et al. 1981; 6 = Piriou and Arashi 1980; 7 = Lazarev 1972; 8 = Handke et al. 1984; 9 = Handke 1984.
* Very strong (Vs), strong (s), and calculated (c) fundamental symmetric (ν_s) or antisymmetric (ν_{as}) stretching vibrations of silicate units (N/A means the band is identified but unassigned).

derivative of the spectra until a goodness of fit is obtained. We then use crystal chemical data, and previous Raman and IR band interpretations, to assign bands to provisional silicate units. Additionally, this paper evaluates the ability of the IR deconvolution model to quantify the silicate units. We chose to examine the μR–FTIR spectra from a suite of PbO-SiO$_2$ glasses ranging from 25–54 mol% SiO$_2$. Although not naturally occurring, the simple PbO-SiO$_2$ system allows us to understand how silicate structures are manifest in IR spectra. Additionally, as the PbO cation acts as a network former we are able to synthesize glasses to very low silica contents (25 mol%), which increase the possibility of identifying all possible structural units in silicate glasses.

IR STUDIES OF SILICATE GLASSES

There have been extensive IR studies to identify the structural units in phosphate, borate and germanium glasses, and also fine grained clays (Agarwal and Tomozawa 1997; Balan et al. 2001, 2002; Efimov 1996), but there have been only a few attempts to fit bands to the spectra of silicate glasses (e.g., Davis et al. 1996; El-Egili 2003; MacDonald et al. 2000; Walrafen and Samanta 1978). Yet, it would be useful to apply a band fitting method to silicate glass IR spectra and to separate the contributions from discrete silicate units. Maxima in the IR spectra that are identifiable prior to deconvolution are referred to as "peaks," and the

individual deconvolved Voigt-shaped vibrational contributions that are summed to reproduce the spectra are referred to as "bands".

Traditionally, structural information from both absorbance and reflectance IR spectra of silicate glasses has been inferred from the systematic shift of the single "peak" in the ~1100–900 cm^{-1} range (e.g., Agarwal and Tomozawa 1997; Efimov 1996; MacDonald et al. 2000; Silver et al. 1990; Stoch and Sroda 1999). The ~1100 cm^{-1} "peak" maxima shifts to lower wavenumbers with increasing fictive temperature (in aluminosilicate and silica glasses; e.g., Agarwal et al. 1995; Fujita et al. 2003); during leaching studies (e.g., Hamilton et al. 2001; MacDonald et al. 2000) and with decreasing SiO_2 content (e.g., Gaskell 1970; Kubicki et al. 1992; Silver et al. 1990; Stoch and Sroda 1999). The shift in the ~1100–900 cm^{-1} "peak" is caused by a decrease in the average Si-O bond angle in the bulk glass due to decreased polymerization of the glass network (reviewed in King et al. 2004). This is accomplished by breaking Si-O-Si, or bridging oxygen (BO) bonds, to form Si-O-M, or non-bridging oxygen (NBO) bonds where the M refers to cations excluding the tetrahedral ions (e.g., Si^{4+}, Al^{3+}, Fe^{3+}). In this study, we investigate the hypothesis that the ~1100–900 cm^{-1} "peak" itself does not shift, instead the "peak" appears to shift due to relative changes in the intensities and FWHM of several "bands" with finite central positions, and that these bands relate to specific silicate units that have distinct molecular geometries. Until now a systematic procedure for resolving these bands from IR spectra of silicate glasses has not been documented comprehensively.

METHODS

Six PbO-SiO_2 glasses were synthesized with compositions ranging between 25 and 54 mol% SiO_2, encompassing glasses from near-metasilicate (>50 mol% SiO_2) to greater than orthosilicate (<33 mol% SiO_2) compositions. Mixtures of 99.995% pure Pb(II)O and SiO_2 powders were ground in an agate mortar and pestle under ethanol for 30 minutes and dried under a heat lamp. Each mixture was sintered in a platinum crucible for three hours, then re-ground and re-sintered. Following heat treatment, the mixture was then re-ground and melted for two hours at ~200 °C above its determined liquidus temperature (from Geller et al. 1934). The platinum crucible was placed but not submerged into ice water to rapidly quench the sample. The sample was then re-crushed, re-melted, and re-quenched. The glasses were mounted in epoxy in separate holes in an aluminum disk and polished to a 1/4 μm finish with diamond grit. Electron microprobe analyses were performed at the University of Western Ontario on a JEOL JXA-8600 Superprobe to confirm that the glasses were homogenous, the correct composition, and that they contained no crystals.

Specular μR-FTIR measurements of the six PbO-SiO_2 glasses were collected at the University of Western Ontario using a Nexus 670 spectrometer with a Globar source, KBr beamsplitter, and a Nicolet Continuum microscope with a MCT/A detector and a continuous dry air purge. The glasses were analyzed with a 100 × 100 μm beam size over a 450–3000 cm^{-1} wavenumber range using 4 cm^{-1} resolution and 200 scans. Background measurements were from a 100% gold slide prior to each glass analysis, and final units were in percent reflectance (%R).

To remove any refractive index effects on the resultant IR spectra, the %R data were smoothed to a 48.212 cm^{-1} window and treated with the Kramers-Kronig relation (following previous workers; e.g., Moore et al. 2000). The Kramers-Kronig relation is used to determine optical constants from IR reflectance spectra, and it is also used to relate reflectance data to absorbance data by enabling the calculation of the absorption coefficient (α).

Specular reflectance spectra are composed of two parts; the refractive index (n) and the dielectric function (ε). Each has a real (n_1, ε_1) and imaginary (n_2, ε_2) component (n_2 is often referred to as the extinction coefficient), and α is related to n_2 by:

$$\alpha = \frac{4\pi n_2}{\lambda} \tag{1}$$

where λ is the wavelength (Hapke 1993). When $\varepsilon = 0$, reflectance (R) is related to n using Fresnel's equation (Hapke 1993):

$$R = \frac{(n-1)^2}{(n+1)^2} \tag{2}$$

when $\varepsilon > 0$ then:

$$\varepsilon = n^2 \tag{3a}$$

and,

$$\varepsilon_1^2 = n_1^2 - n_2^2 \tag{3b}$$
$$\varepsilon_2 = 2n_1 n_2 \tag{3c}$$

The Fresnel Equation 2 is then re-written as:

$$R = \frac{(n_1 - 1)^2 + n_2^2}{(n_1 + 1)^2 + n_2^2} \tag{4}$$

The Kramers-Kronig relation relates n_1 and n_2 to Θ, the loss function or phase change (e.g., Hapke 1993):

$$n_1 = \frac{1 - R}{1 + R - 2\sqrt{R}\cos\Theta} \tag{5a}$$

$$n_2 = \frac{2\sqrt{R}\sin\Theta}{1 + R - 2\sqrt{R}\cos\Theta} \tag{5b}$$

where,

$$\Theta = \frac{1}{2\pi} \int_0^\infty \log\left[\left|\frac{\upsilon + \upsilon*}{\upsilon + \upsilon*}\right|\right] \frac{d\log R(\upsilon*)}{d\upsilon*} d\upsilon \tag{6}$$

and υ is the frequency and $\upsilon*$ is the integration variable at each frequency considered.

Thus, the phase change, due to reflection, may be calculated for any wavenumber and n_1 and n_2 may be reconstructed. The calculated n_2 value for each wavenumber is then used to solve Equation 1 and α is generated from the reflectance data. The reconstructed spectra (in KK absorbance) have the effect from the real refractive index removed, which normalizes the reflectance spectra, enabling the different spectra to be compared directly.

The spectra were manually baseline corrected using multiple linear baselines with nodes at approximately 1230, 830, and 730 cm^{-1} to create a flat background. The spectra were then cropped to the 750–1250 cm^{-1} range because it is between 800–1200 cm^{-1} that the major bands of interest occur. Reflectance spectra that have been smoothed, subjected to the Kramers-Kronig relation, and manually baseline corrected are referred to as the "treated" spectra.

PRELIMINARY APPROACHES TO DEFINING VOIGT BAND CHARACTERISTICS

In the following section, we present a rationale for systematically and logically determining the location and number of Voigt-shaped bands to use in subsequent band fitting analyses. A methodical approach to predicting band characteristics is important to unambiguously assign discrete Si-O bands to specific silicate units.

Band shapes

In liquids and gases, when a molecule is excited the time it takes to relax back to its ground state is known as the lifetime of the vibration, and because this process produces spatially coherent excitations it is accurately described by a Lorentzian distribution (Efimov 1999; Gervais et al. 1987; Hirschmugl 2002; McMillan 1984; McMillan and Wolf 1995). Theoretically the Lorentzian distribution is related to damping coefficients and phonon lifetimes of the vibration (Efimov 1999). However, in solids the vibrational mode of a molecular unit is localized

causing the Lorentzian distribution to broaden and more closely resemble a Gaussian distribution (e.g., Gervais et al. 1987; Hirschmugl 2002).

In amorphous solids, like glasses, the situation is more complicated because we cannot assume spatial coherence (translational symmetry; e.g., Efimov 1999) and it is not clear whether a specific band profile reflects the physics of the vibrational modes in the glass. For glasses, the pure Lorentzian distribution is theoretically inappropriate for describing the vibrational lifetimes of structural units present. Furthermore, the Gaussian distribution is inadequate because it assumes negligible phonon damping (Efimov 1999), which is unlikely in a glass. Despite the difficulties with both Lorentzian and Gaussian distributions for describing the vibrations of structural units in glasses, we propose that a symmetrical combination of the two distribution types is the most appropriate (e.g., Voigt and modified Gaussian model distributions). For internal consistency we chose the Voigt distribution to model the band shapes associated with the vibrations of the structural units in our spectra. The Voigt distribution is used in this study because we have effectively removed the asymmetric refractive index component of each spectrum (using the Kramers-Kronig relation), thus the vibrational lifetime of each silicate unit should be symmetrical. We note that symmetrical band profiles will not accurately describe the spectral features in pure reflectance or emission spectra where instead a modified Gaussian model should be considered (Sunshine et al. 1990).

Evaluation of possible band positions

In this, and any vibrational study, a spectrum of a multi-component sample represents the sum of all vibrational contributions from individual molecules (units), and the purpose of any band-fitting model is to separate overlapping bands in the spectra (e.g., Chen and Garland 2003; Vandeginste and De Gaian 1975). The procedure used to determine the number and position of bands in this study is illustrated in Figure 2, where it is assumed that the center of the bands contributing to the IR spectra remain stationary. The observed wavenumber shift of the Si-O "peak" in this, and other studies, and the observation of inflection points in the spectra indicate that more than one band contributes to the overall spectral shape. To preliminarily constrain the number and position of possible bands to use in the band fitting process we reviewed the number and position of previously published bands from Raman and IR spectra of silicate glasses (Tables 1a and 1b; Fig. 2a). It is not expected that all of the Raman and IR band assignments would correlate since Raman and IR techniques are sensitive to different molecular structures and vibrations (Lazarev 1972; McMillan and Wolf 1995; Wartewig 2003). However, for the silicate vibrational modes that are both Raman- and IR-active (e.g., McMillan and Wolf 1995; Sharma et al. 1997), the Raman bands may be used in this preliminary stage as a guide to the number and position of the IR bands corresponding to those silicate vibrations.

To identify the average position and number of specific overlapping bands in this study we determined the positions of inflections in the treated spectra. The positions of the inflections are highlighted using the derivative of the spectrum (Fig. 2b). We use the second derivative of the spectra, although we
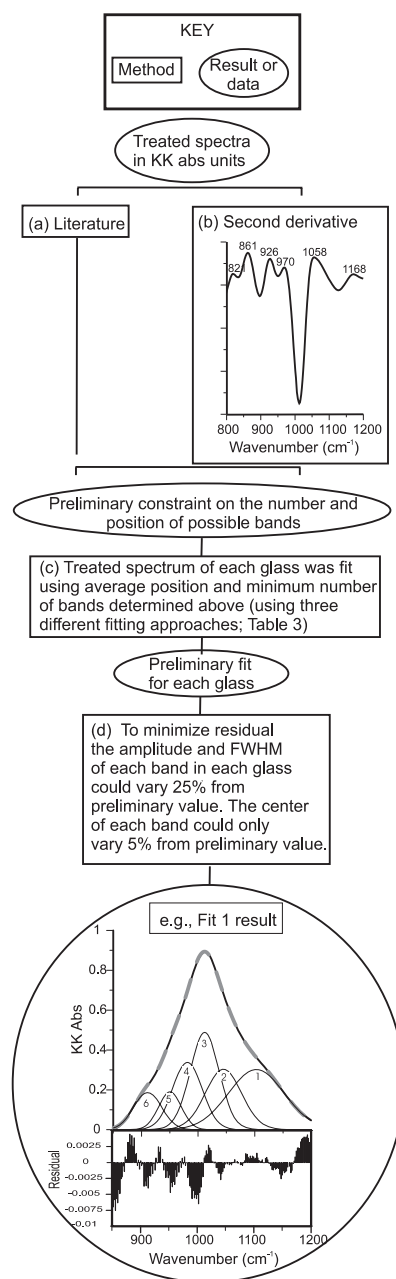

FIGURE 2. Flow chart illustrating the steps taken to deconvolve Voigt-shaped bands from the treated spectra (in all three fitting methods). First, a literature search on the position of Raman and IR bands of silicate glasses (**a**), and the calculation of the second derivative of the spectra (**b**), provided a preliminary constraint on potential band characteristics. The treated spectra were fit with bands at centers close to those predicted from methods **a** and **b** (using three different fitting approaches) to produce preliminary fits (**c**). During the final iteration process (**d**), both the amplitude and FWHM of each band was free to vary with 25% of the amplitude determined in the preliminary fits and the center of each Voigt-shaped band was constrained to within 5% of the center determined in the preliminary fits. The goodness of the resultant fits (Fit 1 illustrated) is monitored using a plot of the residuals, where there was <0.02 KK abs difference between the real and reconstructed spectra.

note that others have also examined the third, fourth, and sixth derivatives (Huguenin and Jones 1986; Scheinost et al. 1998). Similar inflection positions were determined by examining the variance between the different spectra, however the features were less resolved than those determined using the second derivative method and are not discussed here.

Further constraints on the final deconvolution method

For each treated spectrum, Voigt-shaped bands were inserted using the PeakFit V4.11 program (Systat Software Inc. 2002) using the centers of the eight bands determined from the methods described above (literature review and second derivative methods). Initially, for internal consistency, the leading edge at the high wavenumber (low energy) end of the spectra of the most silica rich glass (54 mol% SiO_2) was fit first and subsequent bands were added until a satisfactory fit was obtained with a minimum number of bands (e.g., Mysen et al. 1982a). However, as discussed below other approaches were used to fit the spectra (Fig. 2c).

After the minimum number of bands was determined for each glass, the fit to each treated spectrum (pre-iterative fit) was inadequate and it was necessary to adjust each fit. To do this the Voigt band center, FWHM and amplitude were optimized using a band-fitting algorithm in the PeakFit V4.11 program. The band centers were constrained to within 5% of the value determined in the pre-iterative fit. The FWHM and amplitude of the bands were relatively unconstrained and were free to vary up to 25% between iterations (Fig. 2d). The model was run to 500 iterations or until goodness-of-fit was maximized, whereby there was convergence (<1 standard deviation) between each spectrum and its corresponding fit. Also, the goodness-of-fit was monitored visually using residual plots, where a satisfactory fit produced a random, but minimal residual (<0.02; Fig. 2; Fit 1 result).

RESULTS

Voigt band characteristics

The average positions of the six "peak" maxima identified in the treated spectra display a systematic shift to higher wavenumbers (cm^{-1}) with increasing mol% SiO_2 content (Fig. 3). Five changes in slope were resolved, on average, for a single glass spectrum after taking the second derivative of the treated spectra, between 1200 and 800 cm^{-1}. When all of the glasses are examined there were a total of eight inflections identified in the glass suite (Table 2).

Error evaluation

One concern regarding any fitting method is whether the bands represent "true" vibrational features in the spectra; it is easy to obtain a low residual fit to a spectrum by using many bands that are theoretically meaningless. To evaluate the errors in the proposed fitting model, a variety of approaches may be taken (Hawthorne and Waychunas 1988). We have chosen to assume that the total number of bands identified is correct based on their correspondence with the literature and second derivative calculations, and also we assume that the bands are Voigt-shaped. To evaluate sources of error (2σ) in the model we examine the effects of fit direction on the resultant band parameters. In Fit 1, the bands are added from high wavenumber to low wavenum-
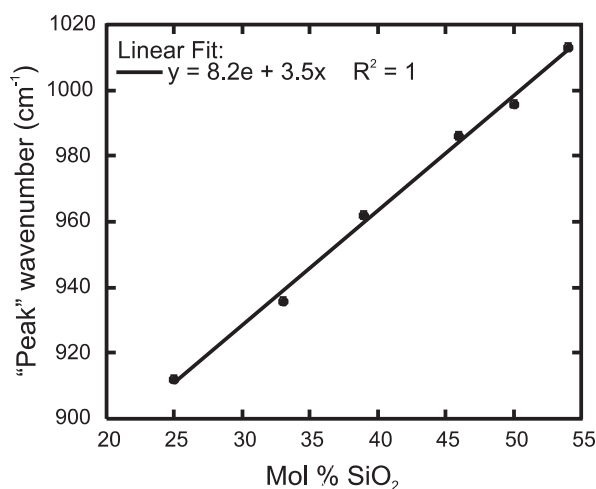

FIGURE 3. The position (cm^{-1}) of the dominant IR "peak" shifts to higher wavenumber in the treated spectra as the mol% SiO_2 of the glass is increased.

ber; in Fit 2 the bands are added from low wavenumber to high wavenumber; and in Fit 3 the bands are added from the highest absorbance location in the spectra to the lowest (i.e., center to wings). In each of the three methods the bands were added at the centers similar to those predicted from the second derivative calculation using the minimum number of bands possible, and no other constraints were imposed. We report the band center (cm^{-1}), amplitude (KK abs), percent area (%KK abs·cm^{-1}), and FWHM (cm^{-1}) of Bands 1 to 8, as a function of glass composition (mol% SiO_2), determined from three different fitting methods (Table 3).

We hypothesized earlier that band centers should not be affected by glass composition and we found that the maximum 2σ in the average band center, within our sample set is 14 cm^{-1} (Band 2, Fit 3; Table 3). In all cases the centers of the eight bands are separated by more than 30 cm^{-1} and therefore we accept the hypothesis that band centers are constant regardless of glass composition and we examine the effect of the fitting methods on the location of the average band center. The maximum difference in average band position, between fitting methods is 12 cm^{-1} (Band 2; Table 3). These results indicate that glass composition and fitting method do not significantly affect the determination of band centers in this study.

Band amplitudes (KK abs) are related to the concentration of the associated structural units in the glass, and therefore we expect band amplitudes to vary as a function of glass composition. To examine how the amplitude of each band is affected by fitting method, we averaged the band amplitude of each band at a single composition over the three fits (Table 3). The associated 2σ of each average is a measure of how the amplitude of a band varies with fitting method. The maximum 2σ between band amplitudes determined for the three fits is 0.34 KK abs (Band 4; 54 mol% SiO_2; Table 3). However, the relative amplitude trends between bands in one glass, and for each band as a function of composition remain the same (Table 3). Therefore, the IR band fitting technique may not be used to derive absolute quantities of silicate units, but it may be used to examine the relative con-

TABLE 2. Predicted number and center position (cm⁻¹) of bands in each glass (25–54 mol% SiO_2) resolved from second derivative calculations

Band no.	8 (cm⁻¹)	7 (cm⁻¹)	6 (cm⁻¹)	5 (cm⁻¹)	4 (cm⁻¹)	3 (cm⁻¹)	2 (cm⁻¹)	1 (cm⁻¹)
Mol% SiO_2								
25		843			986		1045	
33	811	856	904	948		1004		1110
39	813	861	916			1021		1130
46	806	866		931	956	1028		
50	833	860		925	963		1042	
54	821	860		930	970		1058	
Average from								
2ⁿᵈ derv.	817	858	910	934	969	1018	1048	1120
Ave. from three fitting methods	830	866	904	947	981	1013	1051	1100

TABLE 3. Band center (cm⁻¹)/amplitude (KK abs)/percent area (%KK abs·cm⁻¹)/and FWHM (cm⁻¹) calculated from each glass using three different fitting methods

	25 mol% SiO_2	33 mol% SiO_2	39 mol% SiO_2	46 mol% SiO_2	50 mol% SiO_2	54 mol% SiO_2	Ave. center(2σ)
Band Fit 1: Bands added from high to low wavenumber [center (cm⁻¹)/amplitude (KK abs)/area (KK abs·cm⁻¹)/FWHM (cm⁻¹)]							
8	821/0.05/1/24						821
7	858/0.12/7/50	856/0.05/3/61	857/0.05/2/59				857(2)
6	906/0.78/71/86	910/0.64/50/86	908/0.54/38/85	909/0.25/14/63	909/0.33/19/78	910/0.17/7/59	909(3)
5	949/0.18/11/61	949/0.32/17/60	948/0.36/18/60	946/0.25/12/53	950/0.21/9/55	950/0.20/8/52	949(3)
4	980/0.11/6/54	981/0.33/8/59	982/0.52/25/59	981/0.60/34/62	982/0.51/26/66	982/0.27/14/65	981(1)
3	1012/0.07/3/43	1012/0.09/5/55	1011/0.12/6/59	1011/0.23/12/57	1007/0.41/17/58	1010/0.51/26/64	1011(4)
2		1047/0.13/7/60	1047/0.18/11/73	1046/0.27/18/73	1046/0.33/17/68	1045/0.29/18/78	1046(2)
1			1097/0.03/1/36	1103/0.15/11/79	1103/0.2/13/85	1103/0.3/27/113	1102(6)
Band Fit 2: Bands added from low to high wavenumber [center (cm⁻¹)/amplitude (KK abs)/area (KK abs·cm⁻¹)/FWHM (cm⁻¹)]							
8	827/0.10/3/32						827
7	861/0.23/11/45	861/0.19/10/60	864/0.21/9/55				862(4)
6	900/0.70/48/65	902/0.48/25/57	902/0.45/19/50	900/0.19/9/49	894/0.23/11/63	908/0.18/7/52	901(9)
5	943/0.43/27/59	940/0.58/30/57	941/0.63/26/50	942/0.40/20/54	943/0.41/20/64	949/0.31/11/46	943(6)
4	980/0.13/8/60	977/0.44/23/57	977/0.62/24/48	983/0.65/33/55	986/0.50/24/64	983/0.45/5/43	981(8)
3	1010/0.06/3/45	1019/0.15/8/57	1011/0.27/11/50	1018/0.32/16/54	1011/0.42/20/64	1014/0.48/17/45	1014(8)
2		1055/0.09/5/56	1049/0.17/10/69	1054/0.22/12/60	1051/0.25/12/65	1043/0.38/21/69	1050(10)
1			1096/0.03/1/36	1102/0.16/11/70	1102/0.20/13/84	1102/0.31/28/116	1101(6)
Band Fit 3: Bands added from high to low amplitude [center (cm⁻¹)/amplitude (KK abs)/area (KK abs·cm⁻¹)/FWHM (cm⁻¹)]							
8	831/0.13/5/38	833/0.04/1/38					832(3)
7	868/0.32/16/47	865/0.13/6/52	865/0.15/8/60				866(4)
6	908/0.76/51/63	905/0.53/33/68	906/0.35/ 20/69	905/0.22/11/54	898/0.27/13/67	900/0.10/4/50	904(8)
5	946/0.30/15/45	950/0.59/35/65	950/0.53/36/83	945/0.37/18/54	946/0.36/16/60	951/0.32/18/70	948(5)
4	977/0.22/11/46	983/0.25/12/51	982/0.43/25/70	981/0.52/26/55	986/0.43/22/68	977/0.11/5/53	981(7)
3	1014/0.08/3/38	1017/0.15/7/52	1029/0.13/6/57	1011/0.38/21/60	1009/0.51/27/70	1012/0.71/35/63	1015(14)
2		1051/0.11/6/59	1069/0.12/6/65	1052/0.22/12/60	1059/0.23/11/64	1058/0.17/7/53	1058(14)
1				1101/0.17/12/76	1107/0.18/11/82	1097/0.34/32/121	1102(11)
Band Average of the three fitting methods: amplitude (2σ; KK abs)/area (2σ; KK abs·cm⁻¹)							
8	0.09(0.08)/ 3(4)	0.04/1					830(7)
7	0.22(0.20)/11(9)	0.12(0.14)/6(8)	0.14(0.16)/6(7)				862(9)
6	0.75(0.08)/57(25)	0.55(0.19)/36(26)	0.45(0.19)/25(21)	0.22(0.06)/11(5)	0.28(0.10)/14(8)	0.15(0.08)/6(4)	904(8)
5	0.30(0.25)/18(16)	0.50(0.31)/27(18)	0.51(0.27)/27(18)	0.34(0.16)/17(8)	0.32(0.20)/15(11)	0.28(0.14)/12(10)	947(6)
4	0.15(0.12)/8(5)	0.34(0.19)/ 17(11)	0.52(0.18)/25(1)	0.59(0.13)/31(8)	0.48(0.09)/24(4)	0.28(0.34)/11(11)	981(0)
3	0.07(0.03)/3(1)	0.13(0.06)/6(3)	0.17(0.16)/8(6)	0.31(0.15)/16(9)	0.44(0.11)/21(9)	0.57(0.25)/26(18)	1013(5)
2		0.11(0.03)/6(2)	0.15(0.07)/9(5)	0.23(0.05)/14(7)	0.27(0.10)/13(6)	0.28(0.21)/15(15)	1051(12)
1			0.03(0.01)/1(0)	0.16(0.01)/11(1)	0.20(0.02)/12(2)	0.32(0.04)/29(5)	1100(1)

Notes: The average band center (cm⁻¹; 2σ) is determined as a function of glass composition for each fit. The average band amplitude (KK abs; 2σ), percent area (% KK abs·cm⁻¹; 2σ), and center (cm⁻¹; 2σ) are calculated from Fits 1–3.

centration of silicate units.

Percent band area (KK abs·cm⁻¹) is linearly correlated with calculated percent band amplitude (KK abs) regardless of changes in band FWHM (Fig. 4), and the same arguments for evaluating errors in amplitudes apply to evaluating error in band areas. There is a maximum 2σ of 26% KK abs·cm⁻¹ in the determination of the percent area between fits (Band 6, 33 mol% SiO_2; Table 3), however the relative trend in percent band areas is the same between fits, and is also the same as that seen for band amplitude (Table 3). Variations in band FWHM are interpreted to represent changes in the structural order of the silicate unit in the glass (Brawer and White 1975). However, there is no theoretical framework available to evaluate the significance of variations and deviations in the determined FWHM of the bands in these glasses and they are not discussed.

To evaluate which of the three fit processes would result in

the deconvolution of the most meaningful band parameters, it is helpful to discuss the localization of bands in vibrational spectra. We note that localized vibrational modes do not interact with their surrounding environment, and therefore the theoretical shape of localized IR bands would represent the ideal Voigt band shape in the glass. Theoretical calculations predict that high wavenumber vibrations are more localized than low wavenumber vibrations (Bell et al. 1970). Therefore, fitting bands beginning at the high wavenumber edge of IR spectra (Fit 1) may result in more meaningful band parameters than the other two fits, and the results of Fit 1 will be discussed in the following sections.

Spectral deconvolution

Eight band centers were required to fit all six glass compositions, with centers that correspond closely to the centers predicted
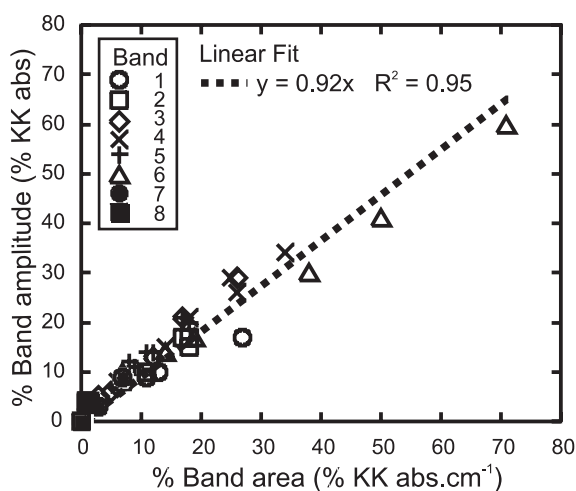
FIGURE 4. Percent band area (%KK abs·cm^{-1}) and percent band amplitude (%KK abs) for Bands 1 to 8 in this study are linearly correlated.

from the second derivative method (Tables 2 and 3). Only six of the eight identified bands were ever used at any one time to fit each IR spectrum, with the exception of the 39 mol% SiO$_2$ glass that required seven bands (Figs. 5a–5f). It is instructive to report changes in the concentration of the bands as a function of composition to evaluate the polymerization state of the glass further on, once the bands have been assigned to silicate units. And although amplitude was discussed earlier as relating to the concentration of structural units, comparing relative band areas is more instructive, and qualitative, because it integrates both amplitude and FWHM characteristics. There were noticeable changes in the area of the bands with varying SiO$_2$ content, and the following section summarizes the behavior of the different Voigt bands from Fit 1 (Figs. 5a–5f; Table 3). The band centers reported in this section are determined by averaging the band centers calculated from the three fitting methods (Table 3).

830 cm^{-1} band: Band 8. The 830 cm^{-1} band occurs only in the spectra of the most PbO-rich glass (25 mol% SiO$_2$), which is the only sample without the 1100 and 1050 cm^{-1} bands (Table 3, Fig. 5f).

860 cm^{-1} band: Band 7. The 860 cm^{-1} band was observed in the spectra of glasses with 25, 33, and 39 mol% SiO$_2$ (Figs. 5d–5f). The area of the 860 cm^{-1} band steadily decreases with increasing SiO$_2$ content, and it never accounts for more than 7% of the spectral area, and it is negatively correlated with the area of Band 1 (Table 3).

900 cm^{-1} band: Band 6. The 900 cm^{-1} band is resolved from all six glass spectra (Figs. 5a–5f), and with respect to area, the 900 cm^{-1} band dominates the 25 mol% SiO$_2$ glass spectra. The area of the 900 cm^{-1} band decreases with increasing SiO$_2$ content of the glass (Table 3).

950 cm^{-1} band: Band 5. The 950 cm^{-1} band increases in area (from 11 to 18%) with increasing SiO$_2$ content from 25 to 39 mol% SiO$_2$ (Table 3). As the SiO$_2$ content of the glass increases from 39 to 54 mol% SiO$_2$ the area of the 950 cm^{-1} band decreases from 18 to 8% (Table 3).

980 cm^{-1} band: Band 4. The area of the 980 cm^{-1} band increases from 6% to 33% as the silica content of the glass is

increased from 25 to 46 mol% SiO$_2$ (Table 3). The 980 cm^{-1} band has the highest band area in the 46 and 50 mol% SiO$_2$ spectra (Figs. 5b and 5c). As the silica content of the glass is increased to 50 mol% SiO$_2$ the area of the 980 cm^{-1} band decreases to 26%, and finally the 980 cm^{-1} band accounts for only 14% of the total spectra at 54 mol% SiO$_2$ (Table 3).

1010 cm^{-1} band: Band 3. The 1010 cm^{-1} band accounts for only 3% of the total area in the 25 mol% SiO$_2$ spectrum, yet the area of the 1010 cm^{-1} band increases with increasing SiO$_2$ content to 26% in the 54 mol% SiO$_2$ spectra (Table 3).

1050 cm^{-1} band: Band 2. The 1050 cm^{-1} band is not detected in the spectra of glasses below 33 mol% in this study, and at this composition the 1050 cm^{-1} band accounts for 7% of the total area of the spectra (Fig. 5e; Table 3). The area of the 1050 cm^{-1} band increases with increasing SiO$_2$ content so that the 1050 cm^{-1} band accounts for 18% of the total area of the 54 mol% SiO$_2$ spectra.

1100 cm^{-1} band: Band 1. Not detected until the 39 mol% SiO$_2$ glass spectra, the 1100 cm^{-1} band accounts for only 1% of the total spectrum area (Fig. 5d; Table 3). As the silica content of the glass is increased to 54 mol% SiO$_2$, the area of the 1100 cm^{-1} band increases so that it is the dominant band at 54 mol% SiO$_2$, accounting for 27% of the total area (Fig. 5a; Table 3).

DISCUSSION

Assignment of silicate units

Previous assignments of silicate units to the bands resolved from Raman and IR spectra of silicate glasses assume that each band represents one vibrational mode specific to only one silicate unit (Table 1a). In contrast this assumption is not used for silicate crystals. In crystals with long-range order a single band may be generated by vibrational modes in different crystal structures (e.g., the 1100 cm^{-1} band is observed in Si$_4$O$_{11}^{6-}$ and SiO$_2$ crystal structures; Table 1b). Whether this kind of behavior is observed in glasses is unknown. And although the peaks in the IR spectra of glasses are much broader than those in crystals with the same stoichiometry (Dowty 1987a, 1987b; McMillan and Wolf 1995), observing the type and positions of the major vibrations in the crystal spectra may help to identify the types of vibrations of the silicate units in glasses. That is, if we assume that the vibrational modes in crystals are similar to those present in glasses, then we may use the position of crystal vibrations to assign silicate units to the bands in the glass.

In the following discussion, we take the simple assumption that the bands that we identified above are caused by discrete silicate unit vibrational modes (Table 1b). We assume that the very strong vibrations contribute significantly to the spectra, and the contributions of strong and/or calculated modes are ignored in the presence of very strong vibrations. By taking this approach we do not intend to suggest that long-range crystalline structures exist in glasses. We note that this approach is not used in other spectroscopic studies because the localization of silicate unit vibrational modes prevents the identification of specific units within different NBO/T groups (e.g., with Raman it is not possible to discriminate between chains and rings; Henderson et al., 1985; McMillan, 1984). As discussed below, the localization of IR vibrational modes is uncertain; therefore it is necessary to test our assumption rigorously. We first assign the eight bands
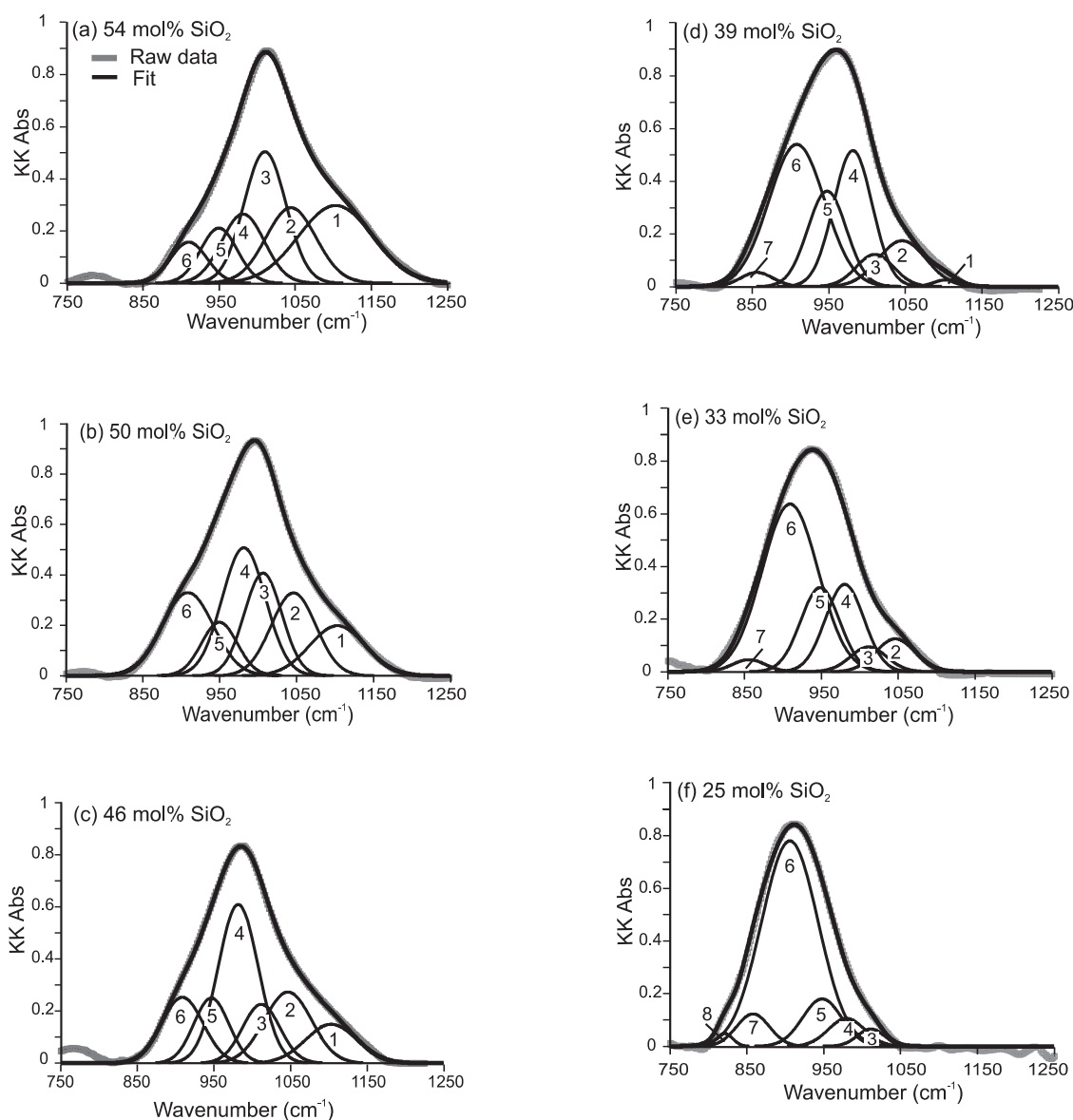
FIGURE 5. The deconvolved bands from Fit 1 (from high to low wavenumber), obtained for the (**a**) 54 mol% SiO$_2$ glass; (**b**) 50 mol% SiO$_2$ glass; (**c**) 46 mol% SiO$_2$ glass; (**d**) 39 mol% SiO$_2$ glass; (**e**) 33 mol% SiO$_2$ glass; and (**f**) 25 mol% SiO$_2$ glass. A total of eight bands were used, at center values (cm^{-1}) within 5% of those predicted from the 2nd derivative of the µR-FTIR spectra.

to eight provisional silicate unit vibrational modes. This data may be used to calculate the relative abundances of the different provisional silicate units in each glass (Table 3). We then assign the eight provisional units to NBO/T groups to further test our assumption by comparing the data to NMR results.

A weak band at ~830 cm^{-1}, generated by weak symmetric stretching (υ_s) SiO$_4^{4-}$ vibrations, has been observed in previous studies (Table 1b). Therefore, the ~830 cm^{-1} band is provisionally assigned to that mode in this study. The 860 cm^{-1} band has one theoretically calculated antisymmetric stretching (υ_{as}) contribution from a SiO$_4^{4-}$-bearing crystal (Table 1b) and is thus provisionally assigned to the vibration of this silicate unit. The 900 cm^{-1} band has only theoretically calculated υ_{as} modes caused by either Si$_2$O$_7^{6-}$ or SiO$_4^{4-}$ units (Table 1b), and this band may not

be unambiguously classified using analogous crystal spectra. The 950 cm^{-1} band may be due to the υ_{as} of either a Si$_6$O$_{18}^{12-}$ or Si$_4$O$_{11}^{6-}$ unit (Table 1b); therefore the 950 cm^{-1} band is not assigned to any one silicate unit using crystal data. The 980 cm^{-1} band has one strong υ_{as} contribution from a Si$_2$O$_6^{4-}$ unit (Table 1b), and so it is provisionally assigned to the υ_{as} vibration of that silicate unit. The 1050 and 1010 cm^{-1} bands have one very strong vibrational mode contribution (from Si$_2$O$_5^{2-}$ and Si$_4$O$_{11}^{6-}$ units respectively; Table 1b), and so the bands are provisionally assigned to the υ_{as} vibration of those silicate units respectively. A very strong υ_{as} mode in the 1100 cm^{-1} range may be generated by either a Si$_4$O$_{11}^{6-}$ or a SiO$_2$ unit (Table 1b), and therefore the 1100 cm^{-1} band cannot be explicitly assigned to a single silicate unit using mineral data.

To determine which structural unit is most likely to contribute to the 1100, 950, and 900 cm^{-1} bands it is instructive to calculate the fundamental frequency produced by any one crystal, and assume that it will be the strongest vibrational mode generated. The fundamental frequency (υ) of a molecular vibration may be approximated assuming the molecule behaves like a simple harmonic oscillator with a spring constant (k) and reduced mass (μ) where:

$$\upsilon = \sqrt{\frac{k}{\mu}} \qquad (7)$$

and wavenumber (cm^{-1}) is υ/speed of light (Herzberg 1945).

Unfortunately the spring constants for all the silicate units illustrated in Figure 1 and Tables 1a and 1b are unknown. However the spring constant is related to bond strength (bs) by Hooke's Law, which in turn is correlated to the charge on the metal cation (M^{m+}) and the number of anions (n) surrounding the cation:

$$bs = \frac{m^+}{n} \qquad (8)$$

In practice, we may not use Equation 8 to calculate actual bond strengths because it does not account for all of the variables that affect bs (e.g., bond length). However, it is useful to calculate the relative bs rank of each of the seven units because it provides a guide as to the numerical sequence of the frequency of vibration for each of the silicate units. The mass and bs of each unit were calculated on a one-Si basis, and the resultant relative bond strengths are reported in Table 4. From Equations 7 and 8, units with a lower bs rank will have a lower vibrational frequency than units with a higher bs rank. When the bs rank and crystal data are combined, it is observed that the relative bs of a $Si_4O_{11}^{6-}$ unit is too low to generate modes in the 1100 cm^{-1} band and too high to generate modes in the 950 cm^{-1} band; and the relative bs of a SiO_4^{4-} unit is too low to generate modes in the 900 cm^{-1} band (Table 4). Therefore, a provisional band assignment is proposed, combining crystal and bs data where: υ_s SiO_4^{4-}(830 cm^{-1}), $\upsilon_{as}SiO_4^{4-}$ (860 cm^{-1}), $\upsilon_{as}Si_2O_7^{6-}$ (900 cm^{-1}), $\upsilon_{as}Si_6O_{18}^{12-}$(950 cm^{-1}), $\upsilon_{as}Si_2O_6^{4-}$ (980 cm^{-1}), $\upsilon_{as}Si_4O_{11}^{6-}$(1010 cm^{-1}), $\upsilon_{as}Si_2O_5^{2-}$ (1050 cm^{-1}), and $\upsilon_{as}SiO_2$ (1100 cm^{-1}; Table 4). The proposed band assignment correlates well with previous Raman and IR interpretations of band positions in other silicate glasses and crystals (Tables 1a and 1b). However, only five bands have been used to fit the previous Raman and IR spectra, where each band is assigned to a silicate unit from one of the five NBO/T groups (Table 1a). In this study eight bands were used to fit the spectra, where two pairs of bands were provisionally assigned to silicate units with the same NBO/T ($Si_2O_5^{2-}$ and $Si_4O_{11}^{6-}$; $Si_2O_6^{4-}$ and $Si_6O_{18}^{12-}$; Table 4), and two bands were attributed to the vibration of a single unit (SiO_4^{4-}; Table 4).

Localization of vibrations

To construct comprehensive models of glass structure, it is necessary to determine how the atoms in the silicate units interact with each other in the glass network. As mentioned earlier, a measure of silicate unit interaction is the degree of localization of their associated vibrational modes. Vibrational modes are localized when they do not interact with their immediate environ-

TABLE 4. The provisional assignment of silicate units to deconvolved bands (cm^{-1}) using a relative bond strength rank

Provisional silicate unit	NBO/T	O per T (Co-ord. No.)	Mass 1-Si basis	Relative bond strength (rank)	Assigned band (~cm^{-1})
SiO_4^{4-}	4	4.00	92	1.00	830
SiO_4^{4-}	4	4.00	92	1.00	860
$Si_2O_7^{6-}$	3	3.50	84	1.14	900
$Si_6O_{18}^{12-}$	2	3.00	76	1.33	950
$Si_2O_6^{4-}$	2	3.00	76	1.33	980
$Si_4O_{11}^{6-}$	1 (and 2)	2.75	72	1.45	1010
$Si_2O_5^{2-}$	1	2.50	68	1.60	1050
SiO_2	0	2.00	60	2.00	1100

Notes: The 1-Si mass was calculated by determining the mass of the unit and dividing it by the number of silicon atoms in the unit formula.

ment, which occurs when there is short- to medium-range order in the glass (Bell et al. 1970). The FWHM of a Voigt band may reflect the degree of interactions between the atoms in the silicate units; however it has been discussed previously that changes in the FWHM of Voigt bands cannot be explicitly compared to the physical nature of the glass at this time. The relative localization of modes has been predicted from the mass and vector displacement of vibrating atoms (Bell et al. 1970), and it was shown that high wavenumber vibrations are more localized than low wavenumber vibrations (Bell et al. 1970). However, it is beyond the scope of this study to calculate how all of the atoms in each silicate unit interact with each other. Further work is required to use this IR technique to evaluate the degree of interaction between the silicate units in the glass structure.

Comparison of the IR results with NMR to evaluate the band assignment

There were five major assumptions made in this deconvolution model to identify the silicate units in the glass. (1) We assume an ionic model of silicate glass structure. (2) Each structural unit has both an IR and Raman active mode (therefore we may use Raman positions to initially place IR bands). (3) There are seven silicate structural units similar to those in silicate crystals. (4) The υ_{as} vibrations of silicate units are similar in position to the strongest modes in silicate crystals. (5) The seven units fall into five NBO/T groups.

We acknowledge that such assumptions may bias the subsequent quantification of silicate units and thus may be used as arguments against using IR to determine the polymerization state of silicate glasses. Therefore, to evaluate the reliability of the assumptions and the results in this study it is helpful to compare it to another method of determining glass structure. Solid state NMR is becoming the most accepted technique used to quantify NBO/T units in glasses at low temperatures and pressures (Eckert 1992; McMillan and Wolf 1995). Percent band amplitude is used in NMR to quantify the relative amounts of identified NBO/T units. It was discussed earlier that the percent area of IR bands is the best measure of silicate unit concentration, however it was also shown that there is a linear relationship between percent band area and percent band amplitude (Fig. 4). Therefore, since percent band amplitude is equivalent to the relative silicate unit concentration in both techniques, it is instructive to compare the quantitative results of this IR study to previously published ^{29}Si NMR studies of PbO-SiO$_2$ glasses (Fayon et al. 1998).

Five NBO/T groups are represented in the ^{29}Si NMR results

(Fayon et al. 1998) and there are eight bands identified in this study, therefore the percent amplitude of the 1050 cm^{-1} ($Si_2O_5^{2-}$) and 1010 cm^{-1} ($Si_4O_{11}^{6-}$) bands from Fit 1 were summed because they both have a NBO/T = 1; the percent amplitude of the 980 cm^{-1} ($Si_2O_6^{4-}$) and 950 cm^{-1} ($Si_6O_{18}^{12-}$) bands were summed because they both have a NBO/T = 2; and the percent amplitude of the 860 and 830 cm^{-1} bands were summed because they belong to different vibrations of the SiO_4^{4-} unit (NBO/T = 4). The observation that more than one silicate unit may have the same NBO/T has been reported from other NMR results (Eckert 1992).

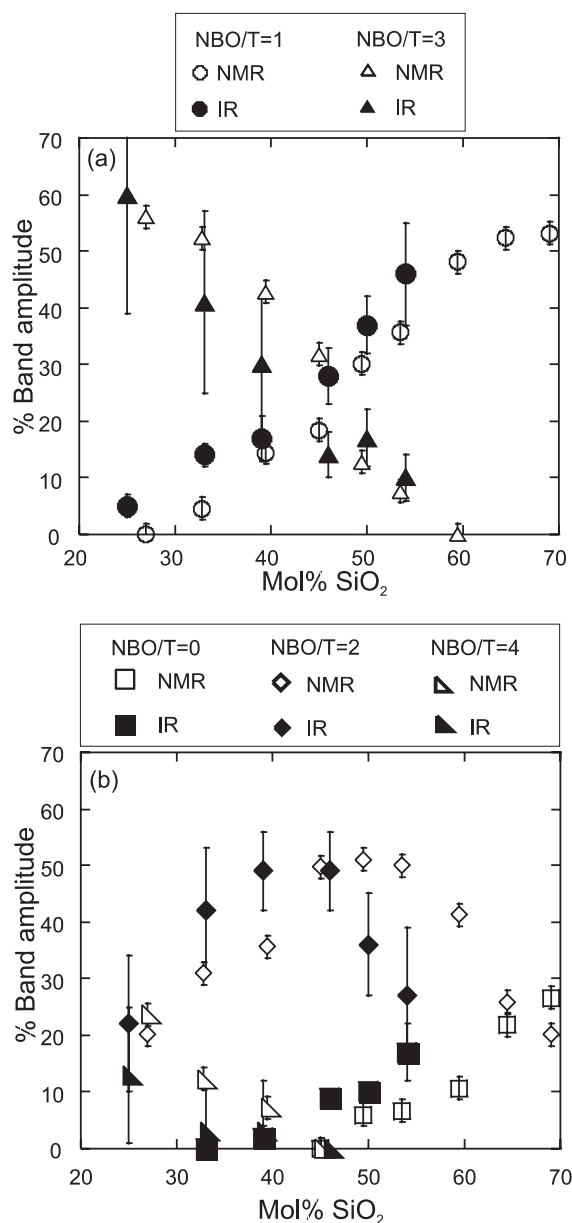The percent silicate unit concentrations (% KK abs) deter-

FIGURE 6. The trends between relative band amplitude and glass composition (mol% SiO_2) determined in this study for (**a**) NBO/T = 1 and 3 units, and (**b**) NBO/T = 0, 2, and 4 units, using FTIR (% KK abs; open symbols) correlate well to trends observed from previously published ^{29}Si NMR data (% Intensity; closed symbols; from Fayon et al. 1998).

mined from this study generally parallel the trends displayed in ^{29}Si NMR results (Fig. 6). Overall, the correlation between the two methods is better at higher SiO_2 contents for NBO/T = 1, 3, and 4 groups (Figs. 6a and 6b). The NBO/T = 0 groups are predicted to exist to lower SiO_2 contents in the IR model compared to ^{29}Si NMR (Fig. 6b). The maximum concentration of NBO/T = 2 groups is shifted to higher SiO_2 contents in the IR results compared to ^{29}Si NMR (Fig. 6b).

The small differences between the two techniques could be accounted for by three sources of error in both IR and ^{29}Si NMR experiments and subsequent interpretations. Firstly, the effective quench rates of the glasses synthesized in both studies are unknown; however quench rates affect the concentration of structural units present in silicate glasses (Stebbins 1995). Second, the band assignments, and underlying assumptions, made in this study may not in detail be correct. For example, perhaps more than one vibrational mode from more than one silicate unit is contributing to the area of one band that would cause an over- or underestimation of band areas. Thirdly, the free induction decay (FID) that occurs during dead time in ^{29}Si NMR analysis could lead to over quantification of silicate units, especially SiO_4^{4-} structures (NBO/T = 4; Eckert 1992).

Despite small differences in the quantification of silicate units in the glass between IR and ^{29}Si NMR methods, the following trends are prevalent in silicate unit concentration as a function of glass composition: The concentration of the NBO/T = 0 and 1 units increases with increasing SiO_2 (Figs. 6a and 6b). The concentrations of the NBO/T = 3 and 4 units decrease with increasing SiO_2 (Figs. 6a and 6b). In both the IR and NMR results, the maximum concentration of NBO/T = 2 units correlates with the first detection of the NBO/T = 0 unit (39 mol% in IR spectra, and 50 mol% in NMR; Fig. 6b). Until the appearance of the NBO/T = 0 units, the concentration of the NBO/T = 2 unit increases with increasing SiO_2. After the appearance of the NBO/T = 0 unit the concentration of the NBO/T = 2 unit decreases as the silica content of the glass is increased (Fig. 6b). These trends are consistent with polymerization trends identified in, and calculated for, other silicate glasses (Maekawa et al. 1991).

REFERENCES CITED

Agarwal, A. and Tomozawa, M. (1997) Correlation of silica glass properties with the infrared spectra. Journal of Non-Crystalline Solids, 209, 166–174.

Agarwal, A., Davis, K., and Tomozawa, M. (1995) A simple IR spectroscopic method for determining fictive temperature of silica glasses. Journal of Non-Crystalline Solids, 185, 191–198.

Balan, E., Saitta, A., Mauri, F., and Calas, G. (2001) First-principles modeling of the infrared spectrum of kaolinite. American Mineralogist, 86, 1321–1330.

Balan, E., Saitta, A., Mauri, F., and Lemaire, C., and Guyot, F. (2002) First-principles calculation of the infrared spectrum of lizardite. American Mineralogist, 87, 1286–1290.

Bell, R., Bird, N., and Dean, P. (1968) The vibrational spectra of vitreous silica, germania and beryllium fluoride. Journal of Physics C: Solid State Physics, 1, 299–303.

Bell, R., Dean, P., and Hibbins-Butler, D.C. (1970) Localization of normal modes in vitreous silica, germania and beryllium fluoride. Journal of Physics C: Solid State Physics, 3, 2111–2118.

Bessada, C., Massiot, D., Coutures, J., Douy, A., Coutures, J.-P., and Taulelle, F. (1994) ^{29}Si MAS-NMR in lead silicates. Journal of Non-Crystalline Solids, 168, 76–85.

Brawer, S. and White, W. (1975) Raman spectroscopic investigation on the structure of silicate glasses. I. The binary alkali silicates. Journal of Chemical Physics, 63, 2421–2432.

Chen, L. and Garland, M. (2003) Computationally efficient curve-fitting procedure for large two-dimensional experimental infrared spectroscopic arrays using the Pearson VII Model. Applied Spectroscopy, 57, 331–337.

Cormier, L., Creux, S., Galoisy, L., Calas, G., and Gaskell, P. (1996) Medium range order around cations in silicate glasses. Chemical Geology, 128, 77–91.

Davis, K., Argarwal, A., Tomozawa, M., and Hirao, K. (1996) Quantitative infrared spectroscopic measurements of hydroxyl concentrations in silica glass. Journal of Non-Crystalline Solids, 203, 27–36.

Dowty, E. (1987a) Vibrational interactions of tetrahedra in silicate glasses and crystals: II. Calculations on melilites, pyroxenes, silica polymorphs and feldspars. Physics and Chemistry of Minerals, 14, 122–138.

——— (1987b) Vibrational interactions of tetrahedra in silicate glasses and crystals: III. Calculations on simple sodium and lithium silicates, thortveitite and rankinite. Physics and Chemistry of Minerals, 14, 542–552.

Eckert, H. (1992) Structural characterization of non-crystalline solids and glasses using solid state NMR. Progress in NMR spectroscopy, 24, 159–293.

Efimov, A. (1996) Section 1. Optical properties of oxide glasses: Quantitative IR spectroscopy: Applications to studying glass structure and properties. Journal of Non-Crystalline Solids, 203, 1–11.

——— (1999) Vibrational spectra, related properties, and structure of inorganic glasses. Journal of Non-Crystalline Solids, 253, 95–118.

El-Egili, K. (2003) Infrared studies of Na_2O-B_2O_3-SiO_2 and Al_2O_3-Na_2O-B_2O_3-SiO_2 glasses. Physica B: Condensed Matter, 325, 340–348.

Fayon, F., Bessada, C., Massiot, D., Farnan, I., and Coutures, J. (1998) ^{29}Si and ^{207}Pb NMR study of local order in lead silicate glasses. Journal of Non-Crystalline Solids, 232–234, 403–408.

Fayon, F., Landron, C., Sakurai, K., Bessada, C., and Massiot, D. (1999) Pb^{2+} environment in lead silicate glasses probed by Pb-L_{III} edge XAFS and ^{207}Pb NMR. Journal of Non-Crystalline Solids, 243, 39–44.

Fujita, S., Sakamoto, A., and Tomozawa, M. (2003) Letter to the editor: Fictive temperature measurement of alumino-silicate glasses using IR spectroscopy. Journal of Non-Crystalline Solids, 330, 252–258.

Furukawa, T., Brawer, S., and White, W. (1978) The structure of lead silicate glasses determined by vibrational spectroscopy. Journal of Materials Science, 13, 268–282.

Furukawa, T., Fox, K., and White, W. (1981) Raman spectrographic investigation of the structure of silicate glasses. III. Raman intensities and structural units in sodium silicate glasses. Journal of Chemical Physics, 75, 3226–3237.

Gaskell, P. (1970) Vibrational spectra of simple silicate glasses. Discussions of the Faraday Society, 50, 82–93.

Geller, R., Creamer, A., and Bunting, E. (1934) The system PbO:SiO_2. National Bureau of Standards, Research Paper RP705, 13, 237–244.

Gervais, F., Blin, A., Massiot, D., Coutures, J., Chopinet, M., and Naudin, F. (1987) Infrared reflectivity spectroscopy of silicate glass. Journal of Non-Crystalline Solids, 89, 384–401.

Hamilton, J., Brantley, S., Pantano, C., Criscenti, L., and Kubicki, J. (2001) Dissolution of nepheline, jadeite and albite glasses: Toward better models for aluminosilicate dissolution. Geochimica et Cosmochimica Acta, 65, 3683–3702.

Handke, M. (1984) Force constants and chemical bond character in (SiO_4) and (GeO_4) anions in orthosilicate and orthogermanates. Journal of Molecular Structure, 114, 187–190.

Handke, M., Kosinsko, K., and Tarte, P. (1984) Vibrational spectra and force constants calculations of the isotopic species of $MgCaSiO_4$. Journal of Molecular Structure, 115, 401–404.

Hapke, B. (1993) Theory of reflectance and emittance spectroscopy, 455 p. Cambridge University Press.

Hawthorne, F. and Waychunas, G. (1988) Spectrum-Fitting Methods. In F. Hawthorne, Ed., Spectroscopic Methods in Mineralogy and Geology, 18, p. 63–98. Reviews in Mineralogy, Mineralogical Society of America, Chantilly, Virginia.

Heaton, H. and Moore, H. (1957) A study of glasses consisting mainly of the oxides of elements of high atomic weight. Part II. The sources of the infra-red absorption bands observed in the transmission curves of the glasses. Journal of the Society of Glass Technology, 41, 28–71.

Henderson, G.S., Bancroft, G.M., and Fleet, M.E. (1985) Raman spectra of gallium and germanium substituted silicate glasses: variations in intermediate range order. American Mineralogist, 70, 946–960. Herzberg, G. (1945) Infrared and Raman spectra of polyatomic molecules. 632 p. Van Nostrand Reinhold Company.

Hess, P. (1975) PbO-SiO_2 melts: structure and thermodynamics of mixing. Geochimica et Cosmochimica Acta, 39, 671–687.

——— (1989) The Nature of Silicate Melts. In P. Hess, Ed., Origin of Igneous Rocks, p. 59–72; 316–329. Harvard University Press, Boston.

Hirschmugl, C. (2002) Frontiers in infrared spectroscopy at surfaces and interfaces. Surface Science, 500, 577–604.

Huguenin, R.L. and Jones, J.L. (1986) Intelligent information extraction from reflectance spectra: Absorption band positions. Journal of Geophysical Research, 91, 9585–9598.

King, P.L., McMillan, P., and Moore, G. (2004) Infrared spectroscopy of silicate glasses with application to natural systems. In P.L. King, M.S. Ramsey, and G.A. Swayze, Eds., Infrared Spectroscopy in Geochemistry, Exploration Geochemistry, and Re-

mote Sensing, Short Course 33, p. 93–133. Mineralogical Association of Canada.

Kubicki, J., Hemley, R., and Hofmeister, A. (1992) Raman and infrared study of pressure-induced structural changes in $MgSiO_3$, $CaMgSi_2O_6$, and $CaSiO_3$ glasses. American Mineralogist, 77, 258–269.

Lazarev, A.N. (1972) Vibrational Spectra and Structure of Silicates. 302p. Consultants Bureau.

MacDonald, S., Schardt, C., Masiello, D., and Simmons, J. (2000) Dispersion analysis of FTIR reflection measurements in silicate glasses. Journal of Non-Crystalline Solids, 275, 72–82.

Maekawa, H., Maekawa, T., Kawamura, K., and Yokokawa, T. (1991) The structural groups of alkali silicate glasses determined from ^{29}Si MAS NMR. Journal of Non-Crystalline Solids, 127, 53–64.

Masson, C.R., Smith, I.B., and Whiteway, S.G. (1970) Activities and ionic distributions in liquid silicates: Application of polymer theory. Canadian Journal of Chemistry, 48, 1456–1464.

McMillan, P.F. (1984) Structural studies of silicate glasses and melts-applications and limitations of Raman spectroscopy. American Mineralogist, 69, 622–644.

McMillan, P.F. and Wolf, G. (1995) Vibrational spectroscopy of silicate liquids. In J. Stebbins, P. McMillan, and D. Dingwell, Eds., Structure, Dynamics and Properties of Silicate Melts, 32, p. 247–315. Reviews in Mineralogy, Mineralogical Society of America, Chantilly, Virginia.

Moore, G., Chizmeshya, A., and McMillan, P. (2000) Calibration of a reflectance FTIR method for the determination of dissolved CO_2 concentration in rhyolitic glasses. Geochimica et Cosmochimica Acta, 64, 3571–3579.

Mysen, B., Finger, L., Virgo, D., and Seifert, F. (1982a) Curve fitting of Raman spectra of silicate glasses. American Mineralogist, 67, 686–695.

Mysen, B., Virgo, D., and Seifert, F. (1982b) The structure of silicate melts: Implications for chemical and physical properties of natural magma. Reviews of Geophysics and Space Physics, 20, 353–383.

Nesbitt, W.H. and Fleet, M. (1981) An ion-association model for PbO-SiO_2 melts: Interpretation of thermochemical, conductivity, and density data. Geochimica et Cosmochimica Acta, 45, 235–244.

Piriou, B. and Arashi, H. (1980) Raman and infrared investigations of lead silicate glasses. High Temperature Science, 13, 299–313.

Poe, B., McMillan, P., Angell, C., and Sato, R. (1992) Al and Si coordination in SiO_2-Al_2O_3 glasses and liquids: A study by NMR and IR spectroscopy and MD simulations. Chemical Geology, 96, 333–349.

Rybicki, J., Rybicka, A., Witkowska, A., Bergmanski, G., Di Cicco, A., Minicucci, M., and Mancini, G. (2001) The structure of lead-silicate glasses: Molecular dynamics and EXAFS studies. Journal of Physics: Condensed Matter, 13, 9781–9797.

Scheinost, A., Chavernas, A., Barron, V., and Torrent, J. (1998) Use and limitations of second-derivative diffuse reflectance spectroscopy in the visible and near-infrared range to identify and quantify Fe oxide minerals in soils. Clays and Clay Minerals, 46, 528–536.

Sharma, S., Cooney, T., Wang, Z., and van der Laan, S. (1997) Raman band assignments of silicate and germanate glasses using high-pressure and high-temperature spectral data. Journal of Raman Spectroscopy, 28, 697–709.

Silver, L., Ihinger, P., and Stolper, E. (1990) The influence of bulk composition on the speciation of water in silicate glasses. Contributions to Mineralogy and Petrology, 104, 142–162.

Stebbins, J. (1995) Dynamics and structure of silicate and oxide melts: Nuclear Magnetic Resonance studies. In J. Stebbins, P. McMillan, and D. Dingwell, Eds., Structure, Dynamics and Properties of Silicate Melts, 32, p. 191–246. Reviews in Mineralogy, Mineralogical Society of America, Chantilly, Virginia.

Stoch, L. and Sroda, M. (1999) Infrared spectroscopy in the investigation of oxide glass structure. Journal of Molecular Structure, 511–512, 77–84.

Sunshine, J., Pieters, C., and Pratt, S. (1990) Deconvolution of mineral absorption bands: An improved approach. Journal of Geophysical Research, 95, 6955–6966.

Systat Software Inc. (2002) PeakFit v4.11 for Windows. Richmond, California.

Toop, G. and Samis, C. (1962) Activities of Ions in Silicate Melts. Transactions of the Metallurgical Society of the American Institute of Mining, Metallurgical, and Petroleum Engineers, 224, 878–887.

Vandeginste, B.G.M. and De Gaian, L. (1975) Critical Evaluation of Curve Fitting in Infrared Spectrometry. Analytical Chemistry, 47, 2124–2132.

Walrafen, G. and Samanta, S. (1978) Infrared absorbance spectra and interactions involving OH groups in fused silica. Journal of Chemistry and Physics, 69, 493–495.

Wartewig, S. (2003) IR and Raman Spectroscopy: Fundamental Processing, 175 p. Wiley-VCH, Weinheim.